BIOCHEMISTRY
including biophysical chemistry & molecular biology

Article

pubs.acs.org/biochemistry

Substrate Activation and Conformational Dynamics of Guanosine 5′-Monophosphate Synthetase

Justin C. Oliver,[†,§] Rebecca S. Linger,[‡] Sridar V. Chittur,[†,∥] and V. Jo Davisson*[,†]

[†]Department of Medicinal Chemistry and Molecular Pharmacology, Purdue University, West Lafayette, Indiana 47907, United States
[‡]Department of Pharmaceutical and Administrative Sciences, University of Charleston, Charleston, West Virginia 25304, United States

Supporting Information

ABSTRACT: Glutamine amidotransferases catalyze the amination of a wide range of molecules using the amide nitrogen of glutamine. The family provides numerous examples for study of multi-active-site regulation and interdomain communication in proteins. Guanosine 5′-monophosphate synthetase (GMPS) is one of three glutamine amidotransferases in *de novo* purine biosynthesis and is responsible for the last step in the guanosine branch of the pathway, the amination of xanthosine 5′-monophosphate (XMP). In several amidotransferases, the intramolecular path of ammonia from glutamine to substrate is understood; however, the crystal structure of GMPS only hinted at the details of such transfer. Rapid kinetics studies provide insight into the mechanism of the substrate-induced changes in this complex enzyme. Rapid mixing of GMPS with substrates also manifests absorbance changes that report on the kinetics of formation of a reactive intermediate as well as steps in the process of rapid transfer of ammonia to this intermediate. Isolation and use of the adenylylated nucleotide intermediate allowed the study of the amido transfer reaction distinct from the ATP-dependent reaction. Changes in intrinsic tryptophan fluorescence upon mixing of enzyme with XMP suggest a conformational change upon substrate binding, likely the ordering of a highly conserved loop in addition to global domain motions. In the GMPS reaction, all forward rates before product release appear to be faster than steady-state turnover, implying that release is likely rate-limiting. These studies establish the functional role of a substrate-induced conformational change in the GMPS catalytic cycle and provide a kinetic context for the formation of an ammonia channel linking the distinct active sites.

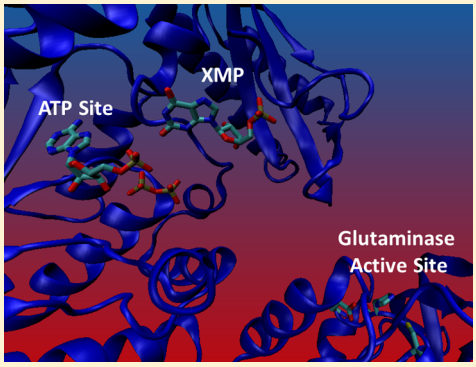

Glutamine amidotransferases (GAT's) catalyze the amination of a wide range of molecules using the amide nitrogen of the side chain of glutamine; these enzymes consist of two domains, one that hydrolyzes glutamine and another that transfers the glutamine-derived ammonia to the waiting acceptor molecule.[1] GMP synthetase (GMPS) is one of three glutamine amidotransferases in *de novo* purine biosynthesis and is responsible for the last step in the guanosine branch of the pathway, the synthesis of GMP via the amination of XMP (Figure 1A).[1,2] The two domains of the *Escherichia coli* enzyme are contained on a single polypeptide, with a class I glutamine amidotransferase domain contained in the first 208 residues and an N-type ATP-PPase domain in the remaining C-terminal segment.

The roles of the GMPS protein domain interactions in the modulation of both catalytic and regulatory functions remain central to understanding the enzyme's broad biological functions. The central role of GMPS in primary metabolism offers examples of selective targeting of antimicrobial therapies.[3] Virulence attenuation in *Mycobacterium tuberculosis* has also generated focus on the mycobacterial GMPS.[4] Furthermore, an antimetabolite therapy-resistant tumor phenotype is linked to downregulation of single-nucleotide point mutations in the GMPS *guaA* gene linked with reduced activation of 6-mercaptopurine and 6-thioguanine.[5,6] The

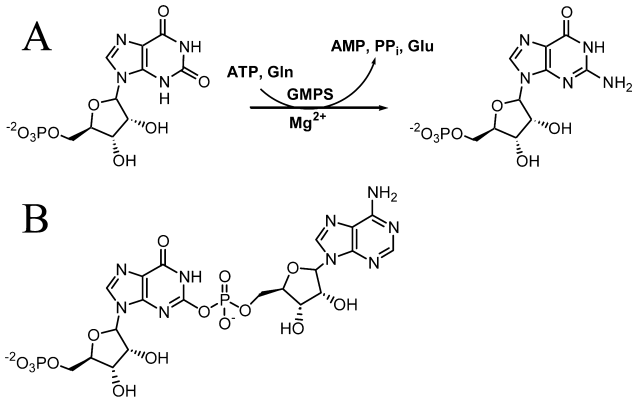

Figure 1. (A) Reaction catalyzed by GMPS. (B) Adenylylated XMP intermediate.

Received: December 27, 2012
Revised: July 8, 2013
Published: July 10, 2013

significance of GMPS continues to emerge, which is exemplified by the recent discovery of an allosteric role in gene regulation through histone deubiquitylation.[7−9]

A common feature of amidotransferase catalysis is an activation step that prepares the acceptor molecule for amination.[10] GMPS belongs to the class of N-type pyrophosphatases, which activate their various substrates by adenylylation.[11] The substrate nucleotide, XMP, is adenylylated on the xanthine C2 oxygen,[12] which is then primed for attack by a nitrogen nucleophile (Figure 1B). A previous study of GMPS demonstrated with positional isotope exchange that adenylylation is a reversible process and, with steady-state techniques, that substrate binding appears ordered, with ATP binding first, XMP second, and glutamine last.[13]

Other common properties of amidotransferases are the conditional glutaminase activities. The glutamine hydrolysis function is not active until a suitable substrate acceptor occupies the distal second domain.[1] Substrate binding leads to a series of conformational changes that propagate through the enzyme and culminate in glutaminase activation; the resulting ammonia is transferred via an intramolecular path to the waiting substrate.[14] While the ammonia tunnel in some related enzyme systems has been elucidated,[15,16] the path between active sites in GMPS has remained undetermined despite the available crystal structures of several forms of the protein, including those from *E. coli*,[17] *Homo sapiens*,[18] and *Pyrococcus horikoshii*.[19] Limitations of these available structural data for GMPS warrant additional biophysical approaches for investigations aimed at addressing functional properties.[17]

Recent studies with related members of the amidotransferase family indicate that once the acceptor substrates bind, these enzymes undergo significant conformational changes.[20−22] These conformational changes are associated with the formation of chambers or tunnels through which the released ammonia can travel between active sites.[23−25] The allosteric steps that modulate glutaminase function continue to be the subject of study across a diverse set of amidotransferases.[26−30] Distinctions within the different amidotransferase families exist, but the mechanisms for maintaining the fidelity of distal coupled activities are emerging.

GMPS has been reported to undergo a conformational change upon binding of its nucleotide substrates alone, without glutamine or other ammonia sources, as indicated by the differential susceptibility to proteolysis or to chemical modification of surface cysteines.[31,32] Using distinct approaches, similar observations were recently made for the *Plasmodium falciparum* form of the enzyme;[33] additional insights regarding glutaminase activation and ammonia utilization by this enzyme have also been recently gained.[34] These studies provided evidence that GMPS can utilize exogenous ammonia in the presence of glutamine, while the exchange of glutamine-derived ammonia with bulk solvent was not observed, indicating the fidelity of the coupled catalytic processes. Even when exogenous ammonia is used as a substrate, there is a dependence on glutaminase and nucleotide acceptor site coupling relayed through the conformational status of the protein.

The details of how the conformational states of GMPS relate to overall turnover events have not yet been established, although nucleotide binding is known to play a role. All current protein crystal structure data implicate a significant global conformational change in the monomeric subunit occurring during ammonia channel formation. This study focuses on single-turnover events associated with the GMPS catalytic cycle to provide insights into the substrate activation and tunnel formation events that occur upon nucleotide binding. Using rapid reaction methodologies for single-turnover experiments, the reaction intermediate of the GMPS reaction has been directly observed. In addition, a conformational change reported through a unique tryptophan residue has been observed during the catalytic cycle. These events have now been temporally aligned with the kinetics of a conformational change that occurs during turnover. The results provide the first complete kinetic cycle through direct observation of intermediate formation, glutamine hydrolysis, and ammonia transfer in an amidotransferase.

EXPERIMENTAL PROCEDURES

Materials. Analytical-grade ATP, glutamine, and EPPS were obtained from commercial sources and used without further purification; commercial XMP was further purified as described previously.[35] Nucleotide concentrations were determined by spectrophotometric measurement of solutions, with reference to published extinction coefficients.[36] Water was processed through a commercial laboratory water purification system before being used.

Protein Purification and Steady-State Assays. *E. coli* GMPS was overexpressed in *E. coli* DH5α and purified as described previously.[37] The enzyme concentration was determined by a dye binding assay,[38] using bovine serum albumin as a standard. The specific activity of purified protein was determined by the direct assay, which continuously follows the 1500 M^{-1} cm^{-1} decrease in the extinction coefficient at 290 nm upon conversion of XMP to GMP.[39] Enzyme preparations were homogeneous as determined by sodium dodecyl sulfate−polyacrylamide gel electrophoresis and by specific activity determinations [typically 40 μmol of GMP min^{-1} (mg of protein)$^{-1}$ (data not shown)]. The turnover number (k_{cat}) of the enzyme was determined by obtaining a substrate saturation curve at 25 °C and fitting the data to the Michaelis−Menten equation with nonlinear curve fitting. For these assays, the glutamine substrate was varied; all others were held at saturating levels. Activity measurements for turnover number determination made use of the direct assay or of the end point glutaminase assay, as described previously.[39,40]

Stopped-Flow Measurements. Stopped-flow measurements were obtained with a Hi-Tech SF-61DX2 instrument, using the single-mixing mode. The temperature was held at 25 °C with a circulating water bath. Absorbance measurements were taken using a 35 W deuterium source and a 1 cm path length configuration. In fluorescence measurements, a 75 W xenon−mercury arc lamp was used; the bandwidth of the excitation light was 2 nm full width at half-height, and emission light was passed through a 320 nm high-pass filter. Instrument control and curve fitting were performed with Hi-Tech KinetAsyst, version 3.

For glutamine-free stopped-flow absorbance measurements, a solution of GMPS and ATP (typically 20 μM and 2 mM, respectively) was rapidly mixed with various concentrations of XMP. In measurements of mixtures containing glutamine, XMP (120 μM) was premixed with the enzyme and ATP at room temperature for 1−3 min before the solution was rapidly mixed with a solution of glutamine (2 mM) and ATP. The concentrations given are those before 1:1 dilution in the stopped-flow device. In all cases, both solutions contained 25 mM EPPS (pH 8.5) and 10 mM $MgCl_2$.

dx.doi.org/10.1021/bi3017075 | *Biochemistry* 2013, 52, 5225−5235

For fluorescence stopped-flow measurements, the enzyme concentration was kept to a final concentration of 0.25 μM to reduce inner-filter effects[35,41] and to achieve pseudo-first-order conditions. The concentrations of other components were maintained at levels given above. All stopped-flow measurements were the average of at least three and up to 20 replicate data collection events per titration point, except the 10 μM point in Figure 7C, which used two replicates. Each event collected 4096 points over the time course of the mixing.

High-Performance Liquid Chromatography (HPLC) Assays. In the analysis of enzyme-bound nucleotide intermediates, solutions for nucleotide−enzyme reactions [typically with 50−100 μM GMPS, 0.5 mM ATP, 200 μM XMP, 20 mM EPPS (pH 8.5), and 10 mM $MgCl_2$] were mixed in a final volume of 100 μL and allowed to equilibrate at room temperature for 1 min before the addition of an internal standard [cytidine 5′-monophosphate (CMP) final concentration of 100 μM] followed by quenching and protein precipitation with ice-cold 50% trichloroacetic acid (2.5% of the final volume). After incubation on ice for 5 min, protein was removed by centrifugation at 15000*g* for 10 min at 4 °C, the supernatant neutralized with 1 μL of 10 N NaOH, and a 25 μL aliquot loaded onto a 4.6 mm × 250 mm (Alltech) or 4.6 mm × 150 mm (Supelco) C18 reversed phase nucleotide separation HPLC column. Separation was achieved using a 1 mL/min flow rate and a linear gradient from 5 to 22% acetonitrile over 10 min and then a steady level of 22% acetonitrile for 15 min; both solvents also contained 50 mM KH_2PO_4 (pH 6.2) and 4 mM tetrabutylammonium phosphate. Detection was accomplished with a diode array detector, monitoring at 220−320 nm. Fractions, collected manually, were heated in a sand bath heated to 100 °C. Separation of authentic nucleotides revealed the following elution times with this solvent system: for the 250 mm column, 5.5 min for CMP, 6.9 min for GMP, 9.8 min for AMP, 13.3 min for XMP, 15.5 min for ADP, and 17.2 min for ATP; for the 150 mm column, 3.4 min for CMP, 4.3 min for GMP, 6.1 min for AMP, 8.6 min for XMP, 10.7 min for ADP, and 12.4 min for ATP.

GMP Synthetase Tryptophan to Phenylalanine Mutants. Tryptophan to phenylalanine mutants were made using the QIAGEN Quickchange site-directed mutagenesis method. Two "mutagenizing" primers (i.e., containing the mutation of interest), complementary to each other, amplified the entire plasmid containing the gene of interest, with the appropriate mutation. A silent mutation that added or removed a restriction site was included in the primers to simplify confirmation of correct plasmid construction. For tryptophan to phenylalanine (W to F) mutagenesis of the GMPS gene, the pET vector harboring the His-tagged *E. coli* GMPS was used as the template (Supporting Information).

The *E. coli guaA* gene contains eight tryptophans, which were removed one at a time using the primers shown in Table S1 of the Supporting Information. The GMPS gene in this plasmid was flanked upstream by an NdeI site and downstream by a HindIII site; in the middle of the gene is a SalI site. Two intermediate plasmids were made by sequential mutagenesis, one containing the first four W to F mutations and another containing the last four. The NdeI−SalI fragment containing the first four mutations and the SalI−HindIII fragment containing the final four were combined onto one plasmid. Recovery of tryptophan at a particular position was achieved by the use of wild-type primers for that position. The mutant proteins were purified as described above for the six-histidine-tagged wild-type protein (Supporting Information). During the final buffer exchange of the protein, tryptophan mutants were observed to precipitate under low-salt conditions, but addition of NaCl to a final concentration of 100 mM eliminated this problem.

RESULTS

Analysis of the Adenylylated XMP Intermediate. An earlier study suggested that the enzyme-bound adenylylated XMP intermediate is stable at least long enough to be separated and analyzed;[12] however, no spectral information, which facilitates the interpretation of the pre-steady-state results below, was reported for the compound. The availability of large amounts of enzyme from a recombinant system[37] facilitated the scale-up of the preparation of the intermediate for analysis. As expected, mixing of GMP synthetase with its nucleotide substrates, in the absence of an ammonia source, led to the formation of a new peak in the HPLC separation of nucleotides from the reaction (Figure 2A, bottom trace); this peak was absent from the enzyme-free controls (data not shown). When the reaction mixture represented in the bottom trace of Figure 2A was treated with glutamine, the new peak disappeared and the reaction product, GMP, appeared (Figure 2A, top trace), consistent with the adenylylated XMP intermediate giving rise to the new peak in the bottom trace. Furthermore, when this new peak was collected and boiled to dryness, it decayed into AMP and XMP (Figure 2B). As the extinction coefficient of AMP is 1.9 times that of XMP at 260 nm,[36] the peak areas of the breakdown products in Figure 2B indicate their presence in a 1:1 molar ratio. The UV−vis spectrum of the adenylylated XMP intermediate is dominated by the adenosine base, with some contribution in the lower ultraviolet from the xanthosine ring (Figure 2C). Attempts to quantify the intermediate by comparing it to the decrease in the level of the substrate were inconsistent, so an estimate of the spectrum of adenylylated XMP has been converted in Figure 2C to millimolar absorptivity using the assumption that the intermediate would have approximately the same maximum as adenosine, which is 15.3 mM^{-1} cm^{-1} at 259 nm.[36] At 290 nm, the millimolar absorptivity of XMP is 4.8 mM^{-1} cm^{-1}, while that of adenylylated XMP is seen to be lower, at approximately 1.2 mM^{-1} cm^{-1} (Figure 2C).

Nucleotide-Only Stopped-Flow Fluorescence Studies. Several lines of study have concluded that GMP synthetase undergoes a significant conformational change upon binding of both of its nucleotide substrates, in the absence of an ammonia source.[39] Indeed, stopped-flow mixing of GMP synthetase (premixed with ATP) with XMP substrate (in the absence of an ammonia source) gives rise to decay in the intrinsic tryptophan fluorescence of the enzyme (Figure 3A). This decay is attributed to a substrate-induced conformational change that alters the environment of one or more of the molecule's eight tryptophans, which are dispersed widely in the structure of the enzyme.[17,33] Although a lag phase is evident in these transients at early time points of <10 ms, too few data points were available to obtain adequate curve fits to this phase. The apparent length of the lag phase did decrease with an increase in the nucleotide substrate concentration, suggesting the delay could be due to nucleotide binding event(s). Time points after the lag phase were modeled by a single-exponential curve of the type shown in eq 1

$$y = -Ae^{-Rt} + C \quad (1)$$

dx.doi.org/10.1021/bi3017075 | *Biochemistry* 2013, 52, 5225−5235

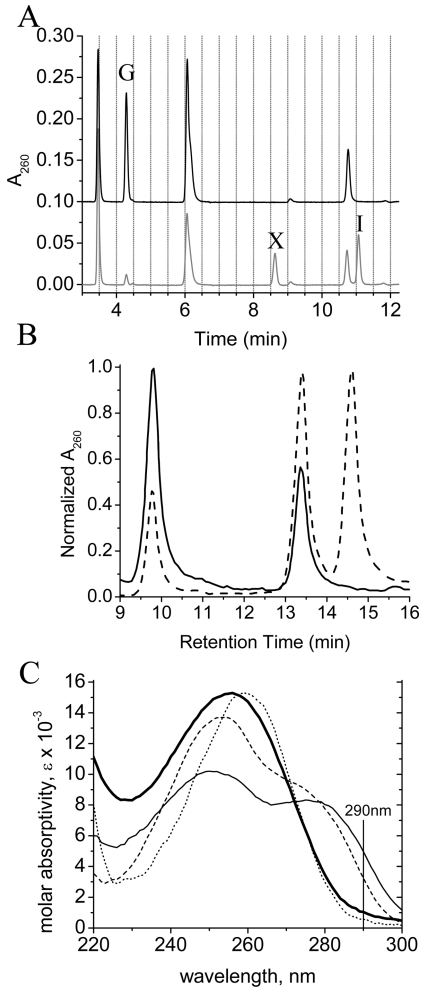

Figure 2. HPLC chromatograms and spectra of nucleotides in the GMPS reaction. (A) Enzymatic conversion of nucleotide intermediate to product. Overlays of nucleotide chromatograms obtained by reaction of enzyme with MgATP and XMP, without an ammonia source (gray, bottom trace) and then by addition of excess glutamine to the same reaction mixture (black, top trace). "I" marks the adenylylated XMP intermediate, "X" XMP, and "G" GMP. The peak at 3.5 min is the CMP internal standard, the peak at 6.1 min AMP, and the peak at 11.2 min ADP (from nonenzymatic hydrolysis of ATP). (B) Decay of the intermediate into its components for nucleotide separations, with AMP at 9.8 min, XMP at 13.2 min, and adenylylated XMP at 14.6 min. The dashed trace shows enzyme-treated nucleotides, without an ammonia source; the sold trace shows the result of collection of the 14.6 min peak and degradation into its components. Peak areas of breakdown products (s-μAU): AMP, 758783; XMP, 385018. (C) Spectra of peaks corresponding to XMP (thin line), GMP (dashed line), AMP (dotted line), and adenylylated XMP (thick line). The GMP spectrum was from a run with authentic GMP, while the other spectra were obtained from runs as in panel A or B.

where A is the amplitude of the change in fluorescence, R is the apparent rate constant, t is time, and C is the calculated final value of the fluorescence. The hyperbolic behavior of the fluorescence decay rate with an increasing XMP concentration (Figure 3B) indicates that the step reported by the signal is a slower unimolecular isomerization or conformational change process occurring after a faster bimolecular binding event.[42] A general mechanism consistent with such a two-step process is given in Scheme 1. In terms of the rate constants given in

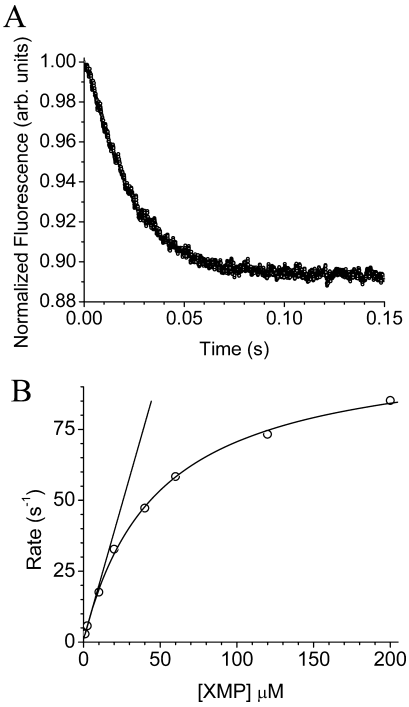

Figure 3. (A) Stopped-flow fluorescence transient observed upon mixing of GMPS-MgATP with XMP (average of four collections). (B) Behavior of fluorescence decay rate with an increasing XMP concentration. The tangent line to the curve at a low substrate concentration is shown.

Scheme 1. General Binding Scheme Consistent with Stopped-Flow Intrinsic Tryptophan Fluorescence Changes Monitored in Mixing of GMP Synthetase with Nucleotide Substrates[a]

$$E + S \underset{k_{-1}}{\overset{k_{+1}}{\rightleftharpoons}} ES \underset{k_{-2}}{\overset{k_{+2}}{\rightleftharpoons}} ES^*$$

[a]The asterisk indicates an isomerization event (e.g., enzyme conformational change). In the case of GMPS, the binding event is fast while the isomerization is slow. E, enzyme; S, substrate.

Scheme 1, the equation describing such hyperbolic rate dependence is given in eq 2[42]

$$k_{app} = k_{-2} + \frac{k_{+2}}{1 + \frac{K_a}{[S]}} \quad (2)$$

where $K_a = k_{-1}/k_{+1}$. Fitting the data in Figure 3B to this equation provides estimates for K_a, k_{+2}, and k_{-2}; a tangent line to the curve at a low substrate concentration provides an estimate for k_{+1}, the apparent second-order rate constant for substrate binding, and therefore also an estimate for k_{-1} (Table 1). The interpretation of the model given above in the context of GMPS nucleotide binding events will be given below, as will the values of the estimates from this model.

Stopped-Flow Fluorescence of Tryptophan to Phenylalanine Mutants. *E. coli* GMPS has a total of eight tryptophan residues, greatly complicating the correlation of tryptophan fluorescence with specific conformational events in the protein. With the goal of simplifying the signal from these residues, several tryptophan to phenylalanine mutants were created. Although not all mutants have so far been generated, preliminary results that shed some light on the substrate-

dx.doi.org/10.1021/bi3017075 | *Biochemistry* 2013, 52, 5225−5235

Table 1. Rate Constants of Nucleotide Activation Steps

step	value	source of data
k_{+1}	2×10^6 M^{-1} s^{-1}	Figure 3B, tangent line
k_{-1}	91 s^{-1}	Figure 3B, curve fit (estimate)
k_{+2}	104 ± 2 s^{-1}	Figure 3B, curve fit
k_{-2}	0.9 ± 0.7 s^{-1}	Figure 3B, curve fit
k_{+3}	40 s^{-1}	Figure 4B, maximal rate (estimate)
k_{-3}	~0.014 s^{-1}	estimate from PIX study[13]
$k_{hydrolysis}$	$\sim 1 \times 10^{-4}$ s^{-1}	Figure 6, curve fit
k_{+4}	$\sim 10^6$ M^{-1} s^{-1}	estimate
k_{-4}	not determined	
k_5	38 s^{-1}	Figure 6B, curve fit rate (estimated to be maximal)
k_6	~7 s^{-1}	rate-limiting step, so approximated by k_{cat}

induced conformational response of the protein were obtained. The mutants discussed here relate to W37 in the protein, which, based on the structure of the enzyme, was thought to offer a position that could be in a "conformational hotspot", where the substrate-induced protein motions would alter the local environment of the residue. A "W37F" mutant was created, in which the W37 position was changed to a phenylalanine. A "37W" mutant was also created, in which all positions except the tryptophan at position 37 were changed to F. Finally, a tryptophan deficient protein was generated, with all the W residues changed to F. Specific activities of the purified mutant proteins are listed in Table 2. Although the mutant

Table 2. *E. coli* GMPS W → F Mutants

protein	specific activity (units/mg)	comment
wild type	24	
W37F	20	
37W	4	soluble in 100 mM NaCl
tryptophan deficient	4	soluble in 100 mM NaCl

proteins are less active than the wild type, they still show significant capacity to turn over substrates, indicative of the overall retention of protein structure and function.

These proteins were examined with stopped-flow fluorescence, using conditions similar to those described earlier for the wild-type protein (Figure 4). For these data, all transients were collected on the same day, consecutively, to minimize differences between the data sets. Clearly, the amplitude and the rate of the fluorescence decay vary with the mutation involved (Table 3). Although the tryptophan deficient mutant showed a slight change in amplitude upon mixing, this decay is not reported in this table. This change is likely the result of fluorescence changes from the remaining tyrosine residues in the protein and represents the background to the predominant tryptophan signal. Tryptophan 37 appears to be the primary reporter of conformational change in the protein, as it alone can lead to the majority of the fluorescence decay seen upon mixing with substrates.

Nucleotide-Only Stopped-Flow Absorbance Studies. Absorbance changes at 290 nm caused by enzyme-catalyzed nucleotide transformations have long been used to monitor the GMPS reaction in the steady state.[39] However, no pre-steady-state observations of these nucleotide absorbance changes have been reported. Rapid mixing of GMPS-ATP with XMP gives rise to a visible decrease in the 290 nm absorbance (Figure 5A). The rate and amplitude of the single-exponential curve fit to

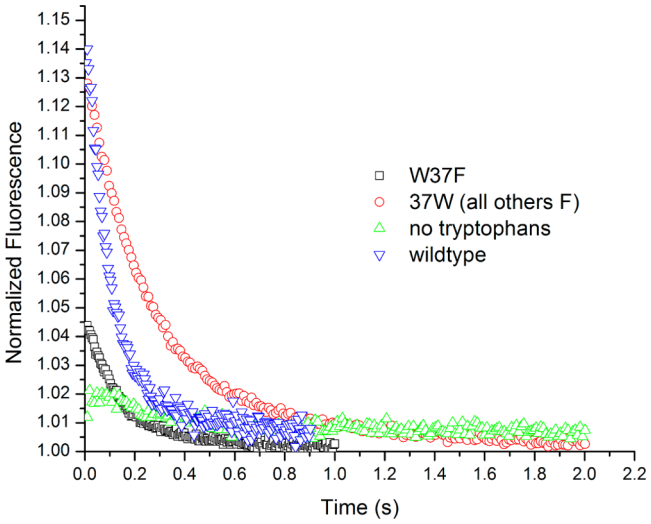

Figure 4. Overlay of stopped-flow fluorescence transients from mixing of *E. coli* GMPS tryptophan mutants with XMP. Mixing condition (final concentrations): GMPS and ATP (1 μM and 1 mM, respectively) and XMP (15 μM). Data normalized to the final fluorescence reading of each data set. Every 20th data point from each transient is shown.

Table 3. Rates and Relative Amplitudes of GMPS Tryptophan Mutants

protein	rate (s^{-1})	amplitude (relative to that of the wild type) (%)
wild type	10.9	100
W37F	8.1	31
37W	4.3	90

this absorbance change were clearly nucleotide concentration-dependent, demonstrating saturation at higher XMP concentrations (Figure 5B). The decline in absorbance reaches a maximal rate of approximately 40 s^{-1}, while at a fixed protein concentration (10 μM), the magnitude of the 290 nm absorbance change reaches a maximum of approximately 3.5×10^{-2}. Concentrations of XMP above 200 μM were not assayed, because GMPS shows substrate inhibition above this level.[35] Similar to the fluorescence data, the behavior of the rate of the absorbance decrease is hyperbolic with an increasing substrate concentration, again implying that the observed change is due to a slow unimolecular step following a fast binding event. Unlike those from the fluorescence experiments, the data in this case were not fit to the hyperbolic function, which requires pseudo-first-order conditions; in most of the absorbance experiments, the reactions do not fulfill this requirement, because XMP substrate concentrations in these experiments ranged from nearly molar equivalence with GMPS to an only 20-fold excess. However, the rate of the absorbance decrease does appear to saturate at a maximum of approximately 40 s^{-1} (Figure 5B,C), independent of the protein concentration, while the magnitude of the decrease in absorbance is proportional to this variable (Figure 5C). A linear regression fit to the absorbance change magnitude versus GMPS concentration data gives a decline in absorbance of 3.1×10^{-3} (μM enzyme)$^{-1}$. The magnitude of the change is consistent with the observed decline in the 290 nm extinction coefficient upon adenylylation of XMP (Figure 2C) and is greater than the magnitude of the conversion of XMP to GMP.[39] The respective values of the nucleotide extinction

dx.doi.org/10.1021/bi3017075 | *Biochemistry* 2013, 52, 5225−5235

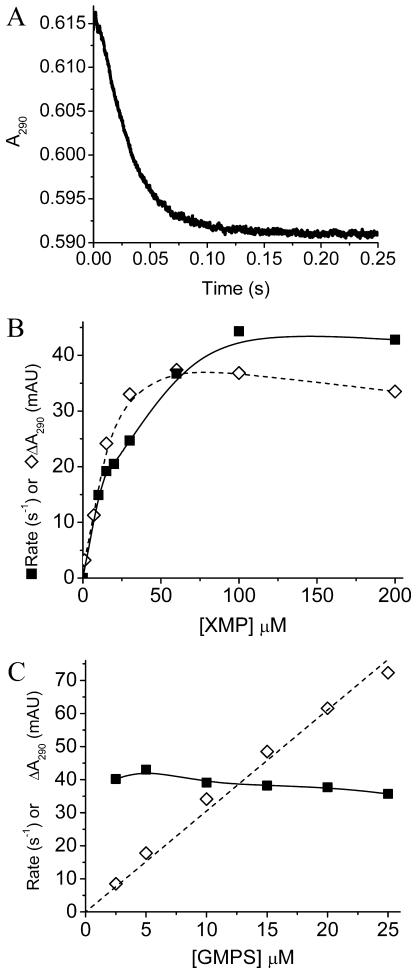

Figure 5. (A) Absorbance transient (290 nm) obtained for the stopped-flow mixing of enzyme with nucleotide substrate only (no ammonia source). GMPS (10 μM), preincubated with ATP (1 mM), was rapidly mixed with XMP (60 μM); both solutions contained 50 mM EPPS (pH 8.5) and 20 mM $MgCl_2$ at 25 °C. All concentrations are those after 1:1 mixing. (B) Behavior of the rate and amplitude of the major absorbance decay seen in panel A, with an increasing XMP concentration: (◇) absorbance decay magnitude and (■) absorbance decay rate. (C) Behavior of the decay, with an increasing enzyme concentration, under saturating nucleotide conditions. Symbols are the same as in panel B.

coefficients are consistent with these results (Figure S1 of the Supporting Information). These observations are consistent with the decrease in absorbance observed upon rapid mixing enzyme with XMP resulting from the chemical conversion of XMP to adenylyl-XMP. Given the observed absorbance changes and estimate of the extinction coefficient for the adenylyl-XMP, 87% occupancy of the enzyme is observed.

Scheme 2 provides a mechanism that describes the kinetic steps occurring as GMPS encounters its nucleotide substrates, in the absence of an ammonia source. In accord with an earlier study,[13] substrate addition is shown as ATP first, followed by XMP; all steps leading up to the adenylylated XMP are shown as being reversible. The initial step of ATP binding is included for the sake of completeness but was not investigated in this work. The two steps defined by k_{+1}, k_{-1}, k_{+2}, and k_{-2} represent the binding of XMP substrate to the enzyme−MgATP complex followed by isomerization and conformational change. Because these steps are consistent with the general model given earlier

Scheme 2. Kinetic Mechanism for Events Occurring When GMPS Encounters Nucleotides (with no ammonia source)[a]

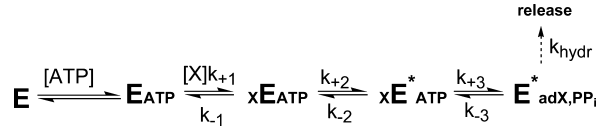

[a]ATP binding is included for the sake of completeness, but it was not monitored in these studies.

for the fluorescence stopped-flow data, k_{+1}, k^{-1}, k_{+2}, and k_{-2} are shared by Schemes 1 and 2. The value calculated for the estimated maximal rate of substrate-induced conformational change, as seen in the fluorescence stopped-flow experiments, is 104 s^{-1} (Table 1), approximately 3-fold greater than the maximal rate of the chemical change, as conveyed by the 290 nm absorbance. The chemical step of adenylylation is therefore reported as a discrete step, k_{+3} (Scheme 2). In addition, an estimate for the rate of the k_{-3} reaction (return of adenylylated XMP to ATP and XMP) is implicit in an earlier positional isotope exchange study of GMPS.[13]

At low ATP concentrations (up to 2-fold molar excess of ATP over protein), the absorbance decays show a different behavior. Over the course of approximately 1 min, the decay returns to the level seen at the start of the mixing (Figure 6). This is consistent with a slow hydrolysis of the adenylylate intermediate to XMP and AMP indicated in Scheme 2 ($k_{hydrolysis}$ in Table 1), a process reported earlier.[13]

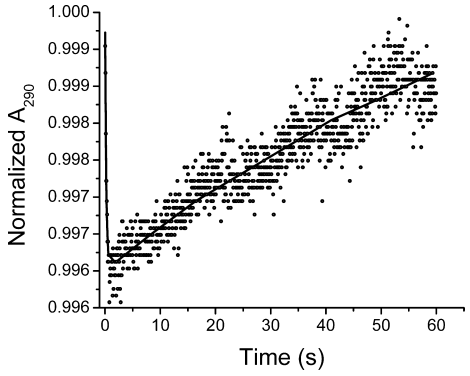

Figure 6. Slow return of A_{290} in GMPS-ATP/XMP stopped-flow mixtures, under conditions of limiting ATP concentrations. Final concentrations are as follows: 10 μM GMPS, 20 μM ATP, and 150 μM XMP.

Stopped-Flow Absorbance Studies with Glutamine. To examine the intrinsic steps in the GMPS reaction in the presence of an ammonia source, stopped-flow mixing of glutamine with the enzyme, premixed with an excess of both nucleotide substrates, was performed. The steps in this case, the binding and hydrolysis of glutamine and the transfer of the resulting ammonia, give rise to rapid absorbance changes. Under conditions where the XMP substrate level is held in molar equivalence with protein, an increase in the 290 nm absorbance is observed, followed by a plateau with no further change (Figure 7A). These absorbance changes are consistent with those expected on the basis of the respective extinction coefficients as stated above (Figure S1 of the Supporting Information).

dx.doi.org/10.1021/bi3017075 | *Biochemistry* 2013, 52, 5225−5235

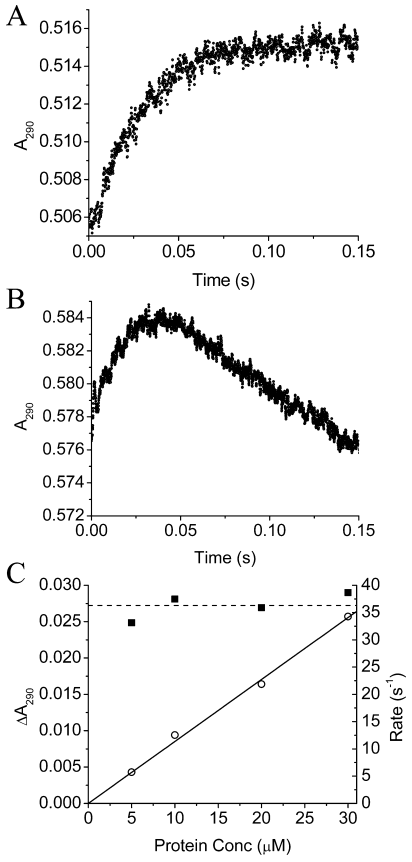

Figure 7. Rapid glutamine-dependent absorbance changes in GMPS turnover. (A) Single-turnover absorbance transient produced by rapid mixing of GMPS-ATP-XMP with excess glutamine and ATP (1 mM each) and limiting XMP (10 μM for both enzyme and XMP). (B) Transient produced under the same mixing conditions as in panel A except for the presence of excess XMP (60 μM). (C) The amplitude of rise depends on protein, whereas the rate does not. The rate of the absorbance rise is shown by filled squares and the calculated amplitude by empty circles. The solid line shows the linear regression to the amplitude data (see the text).

Figure 7B shows the same experiment, except with XMP in excess of protein. As before, the absorbance rise also initially occurs, but in this case, the plateau phase is replaced with a linear decline, consistent with the steady-state conversion of XMP to GMP as exploited for a standard steady-state assay for the enzyme.[39] A very brief lag phase, consistent with glutamine binding, precedes the rise phase in both cases. In the single-turnover case, an increase in the level of the enzyme used in the experiment led to a proportional increase in the amplitude of the rise phase, as determined by a single-exponential curve fit to this phase; however, the rate of the rise stayed within the range of 35–40 s^{-1}, independent of protein concentration (Figure 7C). Taken together with the ultraviolet spectra of adenylylated XMP and GMP, these data are consistent with the glutamine-dependent absorbance rise being due to a burst of conversion of enzyme-bound adenylylated XMP intermediate to GMP.

A kinetic model taking these glutamine-dependent data into account is shown in Scheme 3. In this model, reversible glutamine binding precedes the catalytic step of the enzyme, here represented by k_5, which is comprised also of the glutamine hydrolysis and ammonia transfer, which cannot be resolved by these experiments. Finally, the scheme shows release of products, which regenerates the free enzyme.

Scheme 3. Minimal Kinetic Mechanism for the Glutamine-Dependent Steps in GMP Synthetase Turnover

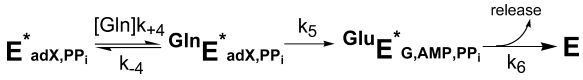

Steady-State Turnover Number. As the steady-state turnover number of *E. coli* GMPS at 25 °C had not been previously reported, the value of this kinetic constant was determined to compare it with the forward rates determined by pre-steady-state methods. Two separate measurements of reaction velocity were taken to arrive at the k_{cat} for the enzyme at 25 °C: a continuous assay monitoring steady-state conversion of XMP to GMP and a glutamine hydrolysis assay, which quantitates the production of glutamate. Both assays produced essentially identical k_{cat} values of 6.9 ± 0.1 s^{-1} (nucleotide conversion) and 7.5 ± 0.1 s^{-1} (glutamate production).

DISCUSSION

Key themes in glutamine amidotransferase catalysis include the upregulation of the catalytic activity of the glutaminase domain by binding of an acceptor substrate in a separate synthetase domain and intramolecular channeling of the glutamine-derived ammonia between distal active sites.[43,44] GMPS demonstrates this conditional glutaminase activity[45] and is also thought to create an ammonia channel via large-scale conformational changes.[17,31] Details of the kinetic and structural events related to channel formation and glutaminase function, however, have been lacking. A feature of GMPS function that proved to be useful in analyzing these details was the sequential and independent nature of the nucleotide activation and the glutamine utilization events allowing separate kinetic investigation of both processes with rapid reaction techniques.

In the kinetic mechanism presented here, a conformational change step follows the fast binding of XMP substrate. The occurrence of a conformational response in GMPS upon substrate binding was noted in an earlier report, which indicated that the enzyme underwent a transition to a compact, protease-resistant structure in the presence of XMP, ATP, and Mg^{2+}.[31] The substrate-induced intrinsic tryptophan fluorescence quenching reported here is consistent with this result and indicates that fast XMP binding is followed by a slower conformational change, estimated to be 104 s^{-1}. For the first time, the conformational transition of this amidotransferase can be correlated with a structural feature in the catalytic cycle. *E. coli* GMPS contains eight tryptophans scattered throughout its structure[46] (Figure S2 of the Supporting Information). The judicious selection of site-directed tryptophan mutants established that the fluorescence transition can be attributed to a large extent to the single W37. Further inspection of the protein structural information regarding this unique position in the *E. coli* GMPS indicates a consistent hypothesis for how this position serves as a suitable reporter of at least a part of the conformational transition (Figure S2 of the Supporting Information). Tryptophan 37 is a nonconserved residue found on the surface of the glutaminase domain of GMPS, near the hinge region of the glutaminase–synthetase interface. In the *E. coli* crystal structure,[17] which is an open conformation of GMPS, the W37 side chain is seen to be in a T-shaped π-stack with F49 (Figure S3 of the Supporting Information). Upon substrate binding, alignment of the domains required to

dx.doi.org/10.1021/bi3017075 | *Biochemistry* 2013, 52, 5225–5235

bring them into the proximity of each other for ammonia transfer requires rearrangement within the region of the W37. As a result of this motion, it is plausible that W37 is exposed to bulk solvent and the intrinsic fluorescence is quenched.

One aspect of the GMPS conformational changes that occur during the catalytic cycle is a large-scale loop disorder-to-order transition to form the complete nucleotide active site. In the *E. coli* GMPS crystal structure,[17] a highly conserved, 22-residue loop was disordered. A crystal structure of human GMPS[47] demonstrated that this region is involved in nucleotide binding with the loop ordered and specific residues interacting with XMP. This region of the protein appears to be crucial for substrate specificity in N-type ATP-pyrophosphatase proteins. For example, in NH_3-dependent NAD^+ synthetase, a substrate-binding and specificity loop was ordered, juxtaposed to its adenylylated nucleotide intermediate.[48] The structures of other family members, such as argininosuccinate synthetase[49] and β-lactam synthetase,[50] also suggest that structurally analogous regions of these proteins are responsible for interaction with their respective substrates.

In GMPS, XMP appears to play a key role in initiating a series of conformational and catalytic events. Upon binding to the protein, the nucleotide induces the transition of the loop to an ordered state. The observation is also corroborated by the earlier proteolysis protection data, because the loop sequence contains three trypsin cleavage sites.[31] Loop closure likely leads to the establishment of a complete binding site for XMP and may also contribute to the formation of an intramolecular ammonia tunnel between the active sites, as in PRPP amidotransferase.[51] The model from the single-turnover studies is consistent with the combination of XMP binding and adenylylation being efficiently coupled to the transmission of the allosteric signal to the distal glutaminase active site.

The available protein crystal structures and the associated biochemical data from the results presented here offer a perspective for analysis of the GMPS active site. In Figure 8 are shown the ligand binding interactions with AMP and XMP in the human GMPS structure. This figure was modeled by aligning the *E. coli* GMPS structure [Protein Data Bank (PDB) entry 1GPM], which has AMP and pyrophosphate bound in the active site, with the human GMPS structure (PDB entry 2VXO), which contains only XMP (Figure S4 of the Supporting Information). The structure for the nucleotide complex indicates a relevant perspective, supported by the proximity of the phosphate of AMP to O2 of XMP (4.2 Å) and to the oxygen of the resultant inorganic phosphate (3.4 Å). These orientations and interatomic distances are consistent with the structure representing the product complex resulting from hydrolysis of the adenylylated XMP.

In Figure 8B, several key protein interactions with the nucleotides and inorganic pyrophosphate are represented, and these interactions summarized in Tables S2 and S4 of the Supporting Information. The numbering given here is that of the *E. coli* enzyme. Residues R308 and F315 reside in α-helix 10, which has been previously described as part of the adenine-specific binding region,[17] and appear to orient the bound AMP. Residues D239 and S240 on α-helix 7, a part of the P-loop common to nucleotide-binding enzymes, function to orient the triphosphate group of ATP in the active site. Adjacent to the P-loop and interacting with D239 is K381, a hydrogen-bonding residue to the pyrophosphate in the crystal structure previously proposed to assist in the orientation of the phosphates of ATP.[17] Lysine 381 is also in the proximity of the synthetase

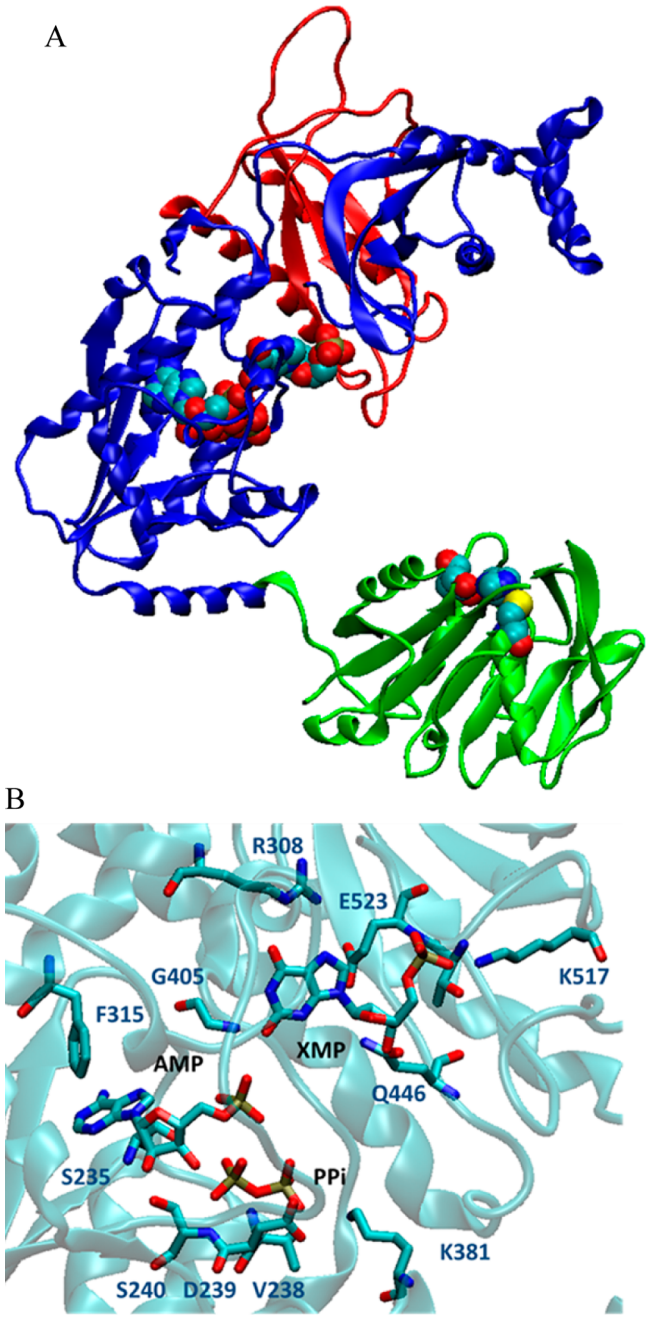

Figure 8. Model of the human GMPS structure (PDB entry 2VXO) with the XMP from the crystal structure and the location of AMP and pyrophosphate from the *E. coli* GMPS (PDB entry 1GPM). The positions of AMP and pyrophosphate were determined by aligning the synthetase domains of PDB entries 2VXO and 1GPM using the structural alignment feature in PyMOL (The PyMOL Molecular Graphics System, version 0.99rc6). (A) Class I glutamine amidotransferase domain (green, residues 1−220), N-type ATP-PPase domain (blue, residues 221−562 and 681−693), and the 118-amino acid insert (red, residues 563−680). In this model, the distance between the C2 oxygen of XMP and the phosphate of AMP is 4.2 Å, indicating that the arrangement of an adenylylated XMP with respect to the protein would be somewhat different than the model hydrolyzed complex shown here. However, the model indicates the approximate position of the nucleotide substrates with respect to the nucleotide-binding loop. (B) Human GMPS (PDB entry 2VXO) with *E. coli* numbering, showing ligand interactions with XMP, AMP, and pyrophosphate.

dx.doi.org/10.1021/bi3017075 | *Biochemistry* 2013, 52, 5225−5235

domain's solvent-exposed surface that faces the glutaminase domain, suggesting a role for conferring to the glutaminase domain the formation of the O^2-adenylyl XMP.

Interdomain residue contacts are expected to play a role in the transmission of the allosteric signal to the glutaminase domain, as observed for IGP synthase.[52] The GMPS conformational changes occurring during the catalytic cycle are interdomain motions that bring the glutaminase and synthetase domains into juxtaposition, a necessity for formation of an intramolecular ammonia path. Despite the human GMPS crystal structure demonstrating the ordered nucleotide-binding loop, no additional structural data have fully captured this path between the active sites, which is a key aspect of glutamine amidotransferases.[30,52] The fluorescence changes reported here suggest that the large-scale conformational changes required to achieve a closed, active enzyme are initiated by XMP binding and adenylylation.

The equilibrium for XMP activation lies far toward the adenylylated form of the substrate. Although this adenylylated intermediate was observed to hydrolyze upon drying, in agreement with an earlier report,[1] it was stable enough in solution to permit, for the first time, collection of a UV spectrum. The intermediate's absorbance at 290 nm is significantly less than that of either the XMP substrate or the GMP product. Combined with the independent, sequential nature of the substrate activation and glutamine utilization reactions, this absorbance difference permitted the monitoring of chemical conversions of nucleotides on the enzyme. The maximal rate of XMP adenylylation by *E. coli* GMPS (40 s^{-1}) is slower than the rate of XMP-induced conformational change by a factor of 2−3. This rate of adenylylation is similar to that seen in other enzymatic adenylylation reactions, for example, in substrate activation in threonyl-tRNA synthetase[53] and tyrosyl-tRNA synthetase.[54]

The rates of events that occur during glutamine utilization were observed by preloading the enzyme with the XMP-adenylylate and subsequent mixing with glutamine. The 38 s^{-1} absorbance increase is attributed to chemical conversion of adenylylated XMP on the enzyme to GMP. This change in the single-turnover absorbance at 290 nm fits a single-exponential function but reports only on the amination of the adenylylated XMP to generate the GMP product. The rate is also similar to those observed in other enzymatic adenylylate turnover reactions, for example, in tyrosyl-tRNA synthetase.[55] However, all steps of glutamine binding, glutamine hydrolysis, and ammonia transfer are included. The lack of an observable time lag suggests that binding and cleavage of glutamine are very fast events with respect to all other steps. In addition, the transfer of ammonia likely occurs at a rate approaching that of free diffusion with a precedent from previously characterized glutamine amidotransferase ammonia tunnels.[51,56,57]

The forward rate constants leading up to and including GMP formation are faster than the steady-state turnover number for the enzyme, determined here to be 7 s^{-1} at 25 °C. This fact is consistent with product release being the rate-controlling step in the overall catalytic cycle and consisting of a slow relaxation of the compact, product-bound conformation back to the open state of the free enzyme. The rate of the ATP binding step was not investigated, for two reasons. First, *E. coli* intracellular concentrations of ATP are likely high enough (~7 mM[58]) under physiological conditions that the binding equilibrium would always be very far toward the bound state. Second, an earlier report indicated that the conformational response of GMPS required the presence of both ATP and XMP nucleotides, while ATP binding alone was insufficient to achieve this response,[31,58] suggesting that the key changes required to activate the enzyme in the ammonia transfer process are elicited by XMP binding. Likewise, a full elaboration of the glutamine-dependent steps was not pursued, for a reason similar to the reason that intracellular glutamine concentrations in enteric bacteria are in the low millimolar range (e.g., ref 59), a condition in which binding of this substrate is also not a rate-limiting process *in vivo*.

In summary, the results reported here provide insights into the detailed mechanism of the substrate-induced cascade that coordinates conformational changes and interdomain signaling in GMPS. The enzyme undergoes a substrate-induced conformational change to a compact state upon nucleotide binding and activation. These XMP-induced changes likely include a large-scale loop disorder to order transition, whole-domain motions, and the transfer of intramolecular signals that activate glutaminase activity in the second domain. The nature of these conformational changes and interdomain signals remains a subject of investigation and will offer important insights into the overall regulation of the catalytic and allosteric properties of N-type ATP-pyrophosphatases and class I glutamine amidotransferases. These features will be ultimately critical to understanding the complex allosteric functions of the additional domain structure occurring in the human enzyme.

■ ASSOCIATED CONTENT

Supporting Information

Additional experimental details for the protein preparations, a table of amino acid residues involved in nucleotide binding, a figure describing the absorbance changes observed in GMPS turnover, two figures highlighting the tryptophan residues in GMPS, and a structural alignment for the nucleotide-binding sites of *E. coli* and human GMPS. This material is available free of charge via the Internet at http://pubs.acs.org.

■ AUTHOR INFORMATION

Corresponding Author

*E-mail: davisson@purdue.edu. Phone: (765) 494-5238.

Present Addresses

[§]J.C.O.: BD Biosciences, 250 Schilling Circle, Cockeysville, MD 21030.

[∥]S.V.C.: Center for Functional Genomics, One Discovery Drive, CRC342G, Rensselaer, NY 12144.

Funding

The research was supported by National Institutes of Health Grants GM067195 (V.J.D.), P20RR016477 (R.S.L.), P20GM103434 (R.S.L.), and T32GM008296 (J.C.O.) and National Science Foundation Grant IGERT 9987576 (J.C.O.).

Notes

The authors declare no competing financial interest.

■ ACKNOWLEDGMENTS

We thank Etti Harms and Nayra Cardenes for preparation of the tryptophan mutant expression plasmids for GMP synthetase.

■ ABBREVIATIONS

CMP, cytidine 5′-monophosphate; EPPS, 4-(2-hydroxyethyl)-piperazine-1-propanesulfonic acid; GMP, guanosine 5′-monophosphate; XMP or X, xanthosine 5′-monophosphate.

REFERENCES

(1) Zalkin, H., and Smith, J. L. (1998) Enzymes utilizing glutamine as an amide donor. *Adv. Enzymol. Relat. Areas Mol. Biol. 72*, 87−144.

(2) Zalkin, H. (1993) The amidotransferases. *Adv. Enzymol. Relat. Areas Mol. Biol. 66*, 203−309.

(3) Rodriguez-Suarez, R., Xu, D., Veillette, K., Davison, J., Sillaots, S., Kauffman, S., Hu, W., Bowman, J., Martel, N., Trosok, S., Wang, H., Zhang, L., Huang, L. Y., Li, Y., Rahkhoodaee, F., Ransom, T., Gauvin, D., Douglas, C., Youngman, P., Becker, J., Jiang, B., and Roemer, T. (2007) Mechanism-of-action determination of GMP synthase inhibitors and target validation in *Candida albicans* and *Aspergillus fumigatus*. *Chem. Biol. 14*, 1163−1175.

(4) Franco, T. M., Rostirolla, D. C., Ducati, R. G., Lorenzini, D. M., Basso, L. A., and Santos, D. S. (2012) Biochemical characterization of recombinant guaA-encoded guanosine monophosphate synthetase (EC 6.3.5.2) from *Mycobacterium tuberculosis* H37Rv strain. *Arch. Biochem. Biophys. 517*, 1−11.

(5) Kudo, M., Saito, Y., Sasaki, T., Akasaki, H., Yamaguchi, Y., Uehara, M., Fujikawa, K., Ishikawa, M., Hirasawa, N., and Hiratsuka, M. (2009) Genetic variations in the HGPRT, ITPA, IMPDH1, IMPDH2, and GMPS genes in Japanese individuals. *Drug Metab. Pharmacokinet. 24*, 557−564.

(6) Karim, H., Hashemi, J., Larsson, C., Moshfegh, A., Fotoohi, A. K., and Albertioni, F. (2011) The pattern of gene expression and gene dose profiles of 6-mercaptopurine- and 6-thioguanine-resistant human leukemia cells. *Biochem. Biophys. Res. Commun. 411*, 156−161.

(7) van der Knaap, J. A., Kumar, B. R. P., Moshkin, Y. M., Langenberg, K., Krijgsveld, J., Heck, A. J. R., Karch, F., and Verrijzer, C. P. (2005) GMP synthetase stimulates histone H2B deubiquitylation by the epigenetic silencer USP7. *Mol. Cell 17*, 695−707.

(8) Faesen, A. C. (2011) Mechanism of USP7/HAUSP activation by its C-terminal ubiquitin-like domain and allosteric regulation by GMP synthetase. *Mol. Cell 44*, 147−159.

(9) Faesen, A. C., Luna-Vargas, M. P., Geurink, P. P., Clerici, M., Merkx, R., van Dijk, W. J., Hameed, D. S., El Oualid, F., Ovaa, H., and Sixma, T. K. (2011) The differential modulation of USP activity by internal regulatory domains, interactors and eight ubiquitin chain types. *Chem. Biol. 18*, 1550−1561.

(10) Massiere, F., and Badet-Denisot, M. A. (1998) The mechanism of glutamine-dependent amidotransferases. *Cell. Mol. Life Sci. 54*, 205−222.

(11) Vetter, I. R., and Wittinghofer, A. (1999) Nucleoside triphosphate-binding proteins: Different scaffolds to achieve phosphoryl transfer. *Q. Rev. Biophys. 32*, 1−56.

(12) Fukuyama, T. T. (1966) Formation of an adenyl xanthosine monophosphate intermediate by xanthosine 5′-phosphate aminase and its inhibition by psicofuranine. *J. Biol. Chem. 241*, 4745−4749.

(13) von der Saal, W., Crysler, C. S., and Villafranca, J. J. (1985) Positional isotope exchange and kinetic experiments with *Escherichia coli* guanosine-5′-monophosphate synthetase. *Biochemistry 24*, 5343−5350.

(14) Raushel, F. M., Thoden, J. B., and Holden, H. M. (2003) Enzymes with molecular tunnels. *Acc. Chem. Res. 36*, 539−548.

(15) Chaudhuri, B. N., Lange, S. C., Myers, R. S., Davisson, V. J., and Smith, J. L. (2003) Toward understanding the mechanism of the complex cyclization reaction catalyzed by imidazole glycerolphosphate synthase: Crystal structures of a ternary complex and the free enzyme. *Biochemistry 42*, 7003−7012.

(16) Thoden, J. B., Holden, H. M., Wesenberg, G., Raushel, F. M., and Rayment, I. (1997) Structure of carbamoyl phosphate synthetase: A journey of 96 Å from substrate to product. *Biochemistry 36*, 6305−6316.

(17) Tesmer, J. J., Klem, T. J., Deras, M. L., Davisson, V. J., and Smith, J. L. (1996) The crystal structure of GMP synthetase reveals a novel catalytic triad and is a structural paradigm for two enzyme families. *Nat. Struct. Biol. 3*, 74−86.

(18) Welin, M., and Nordlund, P. (2010) Understanding specificity in metabolic pathways: Structural biology of human nucleotide metabolism. *Biochem. Biophys. Res. Commun. 396*, 157−163.

(19) Maruoka, S., Horita, S., Lee, W. C., Nagata, K., and Tanokura, M. (2010) Crystal structure of the ATPPase subunit and its substrate-dependent association with the GATase subunit: A novel regulatory mechanism for a two-subunit-type GMP synthetase from *Pyrococcus horikoshii* OT3. *J. Mol. Biol. 395*, 417−429.

(20) Li, A.-A., Mavrodi, D. V., Thomashow, L. S., Roessle, M., and Blankenfeldt, W. (2011) Ligand binding induces an ammonia channel in 2-amino-2-desoxyisochorismate (ADIC) synthase PhzE. *J. Biol. Chem. 286*, 18213−18221.

(21) Mouilleron, S., and Golinelli-Pimpaneau, B. (2007) Conformational changes in ammonia-channeling glutamine amidotransferases. *Curr. Opin. Struct. Biol. 17*, 1−12.

(22) Johnson, J. L., West, J. K., Nelson, A. D. L., and Reinhart, G. D. (2007) Resolving the fluorescence response of *Escherichia coli* carbamoyl phosphate synthetase: Mapping intra- and intersubunit conformational changes. *Biochemistry 46*, 387−397.

(23) Raushel, F. M., Thoden, J. B., and Holden, H. M. (1999) The amidotransferase family of enzymes: Molecular machines for the production and delivery of ammonia. *Biochemistry 38*, 7891−7899.

(24) Weeks, A., Lund, L., and Raushel, F. M. (2006) Tunneling of intermdiates in enzyme-catalyzed reactions. *Curr. Opin. Chem. Biol. 10*, 465−472.

(25) Miles, E. W., Rhee, S., and Davies, D. R. (1999) The molecular basis of substrate channeling. *J. Biol. Chem. 274*, 12193−12196.

(26) De Ingeniis, J., Kazanov, M. D., Shatalin, K., Gelfand, M. S., Osterman, A. L., and Sorci, L. (2012) Glutamine versus ammonia utilization in the NAD synthetase family. *PLoS One 7*, e39115.

(27) Vanoni, M. A., and Curti, B. (2008) Structure-function studies of glutamate synthases: A class of self-regulated iron-sulfur flavoenzymes essential for nitrogen assimilation. *IUBMB Life 60*, 287−300.

(28) Tanwar, A. S., Morar, M., Panjikar, S., and Anand, R. (2012) Formylglycinamide ribonucleotide amidotransferase from *Salmonella typimurium*: Role of ATP complexation and the glutaminase domain in catalytic coupling. *Acta Crystallogr. D68*, 627−636.

(29) List, F., Bocola, M., Haeger, M. C., and Sterner, R. (2012) Constitutively active glutaminase variants provide insights into the activation mechanism of anthranilate synthase. *Biochemistry 51*, 2812−2818.

(30) Amaro, R. E., Sethi, A., Myers, R. S., Davisson, V. J., and Luthey-Schulten, Z. A. (2007) A network of conserved interactions regulates the allosteric signal in a glutamine amidotransferase. *Biochemistry 46*, 2156−2173.

(31) Zyk, N., Citri, N., and Moyed, H. S. (1969) Conformative response of xanthosine 5′-phosphate aminase. *Biochemistry 8*, 2787−2794.

(32) Patel, N., Moyed, H. S., and Kane, J. F. (1977) Properties of xanthosine 5′-monophosphate-amidotransferase from *Escherichia coli*. *Arch. Biochem. Biophys. 178*, 652−661.

(33) Bhat, J. Y., Venkatachala, R., and Balaram, H. (2011) Substrate-induced conformational changes in *Plasmodium falciparum* guanosine monophosphate synthetase. *FEBS J. 278*, 3756−3768.

(34) Bhat, J. Y., Venkatachala, R., Singh, K., Gupta, K., Sarma, S., and Balaram, H. (2011) Ammonia channeling in *Plasmodium falciparum* GMP synthetase: Investigation by NMR spectroscopy and biochemical assays. *Biochemistry 50*, 3346−3356.

(35) Deras, M. L., Chittur, S. V., and Davisson, V. J. (1999) N2-Hydroxyguanosine 5′-monophosphate is a time-dependent inhibitor of *Escherichia coli* guanosine monophosphate synthetase. *Biochemistry 38*, 303−310.

(36) Burton, K. (1969) Spectral data and pK values for purines, pyrimidines, nucleosides, and nucleotides. In *Data for biochemical research* (Dawson, R., Elliott, D., Elliott, W., and Jones, K., Eds.) Clarendon Press, Oxford, U.K.

(37) Tesmer, J. J., Stemmler, T. L., Penner-Hahn, J. E., Davisson, V. J., and Smith, J. L. (1994) Preliminary X-ray analysis of *Escherichia coli* GMP synthetase: Determination of anomalous scattering factors for a cysteinyl mercury derivative. *Proteins 18*, 394−403.

(38) Bradford, M. M. (1976) A rapid and sensitive method for the quantitation of microgram quantities of protein utilizing the principle of protein-dye binding. *Anal. Biochem. 72*, 248−254.
(39) Moyed, H. S., and Magasanik, B. (1957) Enzymes essential for the biosynthesis of nucleic acid guanine:xanthosine 5′-phosphate aminase of *Aerobacter aerogenes*. *J. Biol. Chem. 226*, 351−363.
(40) Zalkin, H. (1985) GMP synthetase. *Methods Enzymol. 113*, 273−278.
(41) Parker, C. A. (1968) *Photoluminescence of solutions. With applications to photochemistry and analytical chemistry*, Elsevier, New York.
(42) Hiromi, K. (1979) *Kinetics of fast enzyme reactions: Theory and practice*, Halstead Press, New York.
(43) Huang, X., Holden, H. M., and Raushel, F. M. (2001) Channeling of substrates and intermediates in enzyme-catalyzed reactions. *Annu. Rev. Biochem. 70*, 149−180.
(44) Chaudhuri, B. N., Lange, S. C., Myers, R. S., Chittur, S. V., Davisson, V. J., and Smith, J. L. (2001) Crystal structure of imidazole glycerol phosphate synthase: A tunnel through a $(\beta/\alpha)_8$ barrel joins two active sites. *Structure 9*, 987−997.
(45) Chittur, S. V., Klem, T. J., Shafer, C. M., and Davisson, V. J. (2001) Mechanism for acivicin inactivation of triad glutamine amidotransferases. *Biochemistry 40*, 876−887.
(46) Tiedeman, A. A., Smith, J. M., and Zalkin, H. (1985) Nucleotide sequence of the guaA gene encoding GMP synthetase of *Escherichia coli* K12. *J. Biol. Chem. 260*, 8676−8679.
(47) Welin, M., Lehtio, L., Andersson, J., Arrowsmith, C. H., Berglund, H., Collins, R., Dahlgren, L. G., Edwards, A. M., Flodin, S., Flores, A., Graslund, S., Hammarstrom, M., Johansson, A., Johansson, I., Karlberg, T., Kotenyova, T., Moche, M., Nilsson, M. E., Nyman, T., Olesen, K., Persson, C., Sagemark, J., Schueler, H., Thorsell, A. G., Tresaugues, L., Van Den Berg, S., Wisniewska, M., Wikstrom, M., and Nordlund, P. (2008) Human GMP Synthetase in Complex with XMP. Protein Data Bank entry 2VXO.
(48) Rizzi, M., Bolognesi, M., and Coda, A. (1998) A novel deamido-NAD^+-binding site revealed by the trapped NAD-adenylate intermediate in the NAD^+ synthetase structure. *Structure 6*, 1129−1140.
(49) Goto, M., Omi, R., Miyahara, I., Sugahara, M., and Hirotsu, K. (2003) Structures of argininosuccinate synthetase in enzyme-ATP substrates and enzyme-AMP product forms: Stereochemistry of the catalytic reaction. *J. Biol. Chem. 278*, 22964−22971.
(50) Miller, M. T., Bachmann, B. O., Townsend, C. A., and Rosenzweig, A. C. (2002) The catalytic cycle of β-lactam synthetase observed by X-ray crystallographic snapshots. *Proc. Natl. Acad. Sci. U.S.A. 99*, 14752−14757.
(51) Krahn, J. M., Kim, J. H., Burns, M. R., Parry, R. J., Zalkin, H., and Smith, J. L. (1997) Coupled formation of an amidotransferase interdomain ammonia channel and a phosphoribosyltransferase active site. *Biochemistry 36*, 11061−11068.
(52) Myers, R. S., Amaro, R. E., Luthey-Schulten, Z. A., and Davisson, V. J. (2005) Reaction coupling through interdomain contacts in imidazole glycerol phosphate synthase. *Biochemistry 44*, 11974−11985.
(53) Bovee, M. L., Pierce, M. A., and Francklyn, C. S. (2003) Induced fit and kinetic mechanism of adenylation catalyzed by *Escherichia coli* threonyl-tRNA synthetase. *Biochemistry 42*, 15102−15113.
(54) Fersht, A. R., Mulvey, R. S., and Koch, G. L. (1975) Ligand binding and enzymic catalysis coupled through subunits in tyrosyl-tRNA synthetase. *Biochemistry 14*, 13−18.
(55) Avis, J. M., Day, A. G., Garcia, G. A., and Fersht, A. R. (1993) Reaction of modified and unmodified tRNA(Tyr) substrates with tyrosyl-tRNA synthetase (*Bacillus stearothermophilus*). *Biochemistry 32*, 5312−5320.
(56) Larsen, T. M., Boehlein, S. K., Schuster, S. M., Richards, N. G., Thoden, J. B., Holden, H. M., and Rayment, I. (1999) Three-dimensional structure of *Escherichia coli* asparagine synthetase B: A short journey from substrate to product. *Biochemistry 38*, 16146−16157.
(57) Amaro, R. E., Myers, R. S., Davisson, V. J., and Luthey-Schulten, Z. A. (2005) Structural elements in IGP synthase exclude water to optimize ammonia transfer. *Biophys. J. 89*, 475−487.
(58) Takesada, H., Ebisawa, K., Toyosaki, H., Suzuki, E. I., Kawahara, Y., Kojima, H., and Tanaka, T. (2000) A convenient NMR method for in situ observation of aerobically cultured cells. *J. Biotechnol. 84*, 231−236.
(59) Ikeda, T. P., Shauger, A. E., and Kustu, S. (1996) *Salmonella typhimurium* apparently perceives external nitrogen limitation as internal glutamine limitation. *J. Mol. Biol. 259*, 589−607.